Journal of Materials Chemistry

Dynamic Article Links

Cite this: *J. Mater. Chem.*, 2011, **21**, 14783

www.rsc.org/materials

PAPER

Immunomagnetic sulfonated hypercrosslinked polystyrene microspheres for electrochemical detection of proteins

Petr Šálek,[a] Lucie Korecká,[b] Daniel Horák,*[a] Eduard Petrovský,[c] Jana Kovářová,[a] Radovan Metelka,[d] Michaela Čadková[b] and Zuzana Bílková[b]

Received 1st June 2011, Accepted 28th July 2011
DOI: 10.1039/c1jm12475g

Poly(styrene-*co*-divinylbenzene) microspheres of narrow size distribution were prepared by (2-hydroxypropyl)cellulose-stabilized dispersion copolymerization of styrene and divinylbenzene in a 2-methoxyethanol/ethanol mixture under continuous addition of divinylbenzene. The copolymerization was initiated with dibenzoyl peroxide. The obtained microspheres were chloromethylated using several chloromethylation agents and then hypercrosslinked. Their porous structure was analyzed by nitrogen adsorption and mercury porosimetry. Superparamagnetic iron oxide nanoparticles were precipitated within the pores of microspheres from Fe(II) and Fe(III) chloride solution. The Fe content in the microspheres was determined by carbon analysis, atomic absorption spectroscopy and thermogravimetric analysis. Magnetic properties of the microspheres were characterized by magnetization curves and the temperature dependence of magnetic susceptibility. Finally, sulfo groups were introduced into the microspheres to prepare an immunomagnetic electrochemical biosensor for protein detection with ovalbumin as a model substance.

Introduction

Separation of polymer or inorganic sorbents from complex mixtures is generally difficult. To alleviate the problem, magnetic microspheres providing large specific surface area (S_{BET}) for covalent binding and narrow size distribution ensuring homogeneous properties were developed. They have been widely used in biological practice, *e.g.*, for protein separation,[1] antibody and enzyme immobilization,[2] cell sorting,[3] nucleic acid[4,5] and protein purification,[6] and in immunoassays.[7] The interest in magnetic separations stems from the fact that they provide easy manipulation and fast isolation using magnetic field; the possibility to obtain desired biological compounds in sufficient purity and concentration necessary for polymerase chain reaction,[8] quantification of biomarkers by mass spectroscopy,[9,10] *etc.* Magnetic microspheres are suitable also as electrochemical biosensors in enzyme-linked immunosorbent assays (ELISA) where the microspheres replace colorimetric end-point measurement. Electrochemical immunosensors based on coupling of immunochemical reactions and appropriate transducers[11] have become attractive due to their simple use, fast analysis and the possibility of miniaturization.[12] Application of magnetic microspheres in immunosensors prevents their poor regeneration and reproducibility, which are often caused by direct adsorption of antibodies on the electrode surface that is commonly used in the immunosensor arrangement.[13] Moreover, screen-printed electrodes (SPEs), which are produced by printing on various polymer or ceramic supports,[14] have advantages of high sensitivity and selectivity, portable size and low cost.

Several methods have been developed to prepare magnetic polymer microspheres including surface-initiated polymerization,[15–17] suspension,[18] dispersion,[19] emulsion,[20] miniemulsion[21,22] and emulsifier-free emulsion[23] polymerization in the presence of magnetic nanoparticles. The magnetic microspheres (size 1–5 μm) have to fulfill requirements for low toxicity (biocompatibility) and non-interference with the chemical environment in diagnostics. Moreover, they should be stable in solutions, show narrow size distribution and minimum non-specific adsorption. Last but not least, an appropriate functionalization of magnetic polymer microspheres is required for intended applications in biochemistry[24] and immunochemistry.[25,26] There is a wide range of different options, such as introduction of basic or acid groups to facilitate desirable adsorption[27] or separation.[28] Ferrites are well known as appropriate magnetic cores of magnetic polymer microspheres. In particular, maghemite and magnetite are often used[29] because of a high saturation magnetization (80–100 A m^2 kg^{-1}). The iron oxides are conveniently prepared in the presence of oleic acid which prevents nanoparticle aggregation in

[a]*Institute of Macromolecular Chemistry, Academy of Sciences of the Czech Republic, Heyrovsky Sq. 2, 162 06 Prague 6, Czech Republic*
[b]*Department of Biological and Biochemical Sciences, Faculty of Chemical Technology, University of Pardubice, Studentská 573, 532 10 Pardubice, Czech Republic*
[c]*Geophysical Institute, Academy of Sciences of the Czech Republic, Boční II/1401, 141 31 Prague 4, Czech Republic*
[d]*Department of Analytical Chemistry, Faculty of Chemical Technology, University of Pardubice, Studentská 573, 532 10 Pardubice, Czech Republic*

organic media.[30] They can be made by precipitation of ferrous and ferric salts with alkali hydroxides[31] or by thermal decomposition of organometal compounds.[32]

Dispersion polymerization has been known as a suitable technique for preparation of monodisperse polymer microspheres in the range 0.1–15 μm.[33] The concentration of monomer and initiator as well as the stabilizer and solvent (hydrocarbon or polar solvent) plays an important role in controlling the microsphere size. Many applications require microspheres crosslinked with another multifunctional monomer to prevent their dissolution in the medium. However, the addition of a crosslinking agent to the reaction system often interferes with the nucleation mechanism of the dispersion polymerization and the resulting particles have then an irregular morphology and a broad size distribution.[34] To overcome this drawback of the polymerization, steric stabilizer or monomer was added to the reaction mixture in several portions[35] or a bifunctional monomer was continuously dosed in certain time periods after beginning of polymerization.[36]

If magnetic nanoparticles are precipitated in the porous structure of polymer microspheres,[37] only limited amounts of a magnetic compound can be incorporated and, moreover, the release of iron oxide from the pores is often a serious problem. For this purpose it is suitable to make the microspheres with micro- (< 2 nm) or mesopores (2–50 nm) in which the iron oxide can be easily kept and thus the incorporated amount of magnetic nanoparticles can be raised. Hypercrosslinking is a convenient method for preparation of micro- and mesoporous microspheres. This reaction was introduced by Davankov in 1970s.[38] Since that time, hypercrosslinked particles have been employed in many fields, such as ion exchangers,[39] water treatment[40] and hydrogen storage.[41] Hypercrosslinked styrene–divinylbenzene copolymers with the size of hundreds of micrometres, so-called Hypersol-Macronet™ sorbent resins, are commercially available from Purolite.[42]

The aim of this work was to investigate the preparation of magnetic polymer microspheres of narrow size distribution from sulfonated hypercrosslinked styrene–divinylbenzene copolymers in which an iron oxide was further precipitated. The microspheres with immobilized anti-OVA antibody were then integrated in a sandwich-type electrochemical immunosensor and ovalbumin was isolated and detected as a model protein (Scheme 1).

Experimental

Materials

Styrene (S) and divinylbenzene (DVB; 54% *meta*- and 20% *para*-isomers, 24% ethylvinylbenzene) from Kaučuk (Kralupy nad Vltavou, Czech Republic) were vacuum distilled; 1,2-dichloroethane (DCE), ethanol (EtOH) for UV spectroscopy, 2-methoxyethanol (MetCel), 25% aqueous solution of ammonia, diethyl ether and cyclohexane were from Lach-Ner (Neratovice, Czech Republic). Chloromethyl methyl ether (CMME), chloromethyl ethyl ether (CMEE), chloromethyl octyl ether (CMOE), (2-hydroxypropyl)cellulose (HPC; M_w = 100 000), $FeCl_2 \cdot 4H_2O$, $FeCl_3 \cdot 6H_2O$, $SnCl_4$ and 2-morpholinoethane-1-sulfonic acid (MES) were from Aldrich (St Louis, USA). Dibenzoyl peroxide (BPO; moistened with 20% of water; crystallized from ethanol), horseradish peroxidase (HRP), chicken egg albumin (ovalbumin, OVA) and bovine serum albumin (BSA) were supplied by Fluka (Buchs, Switzerland). Rabbit anti-ovalbumin (anti-OVA) IgG and rabbit anti-ovalbumin HRP-labeled anti-ovalbumin (anti-OVA-HRP) were obtained from Patricell Ltd. (Nottingham, UK) and purified by affinity chromatography. All other chemicals were supplied by Aldrich or Penta (Chrudim, Czech Republic) and used without further purification.

Preparation of microspheres

Dispersion copolymerization of styrene and divinylbenzene. Poly-(styrene-*co*-divinylbenzene) (PS) microspheres were prepared by modified Ober's procedure.[33] Polymerization was conducted in a glass 100 ml reaction vessel equipped with an anchor-type stirrer. In a typical experiment, HPC (1.09 g) was dissolved in a mixture of MetCel (19.3 g) and EtOH (38.9 g) and separately BPO (0.48 g) was dissolved in S (10.9 g). Both the solutions were mixed and placed in a reaction vessel and purged with nitrogen for 15 min. The reaction was allowed to proceed at 75 °C for 24 h under stirring (100 rpm). Five minutes after the start of the polymerization, DVB (0.11 g; 1 wt%) was added at various rates: 0.11 g in one portion, 2 μl every 30 s for 30 min, 2 μl every 45 s for 45 min, 2 μl every 60 s for 60 min and 2 μl every 75 s for 75 min. At the end of the reaction, the resulting PS microspheres were separated by centrifugation (600 rpm) and washed ten times with ethanol (100 ml each) to ensure complete removal of impurities (excessive stabilizer, unreacted monomer, initiator residues), and finally dried at room temperature.

Preparation of hypercrosslinked PS microspheres. PS microspheres were hypercrosslinked according to the modified Davankov's procedure.[43,44] In a typical experiment, the PS microspheres (2 g) were swollen in anhydrous DCE (32 ml) for 20 h in a 100 ml round-bottomed flask. The mixture was cooled to −15 °C in an ice/NaCl bath under magnetic stirring, chloromethyl methyl ether (0.727 ml) was added and the mixture

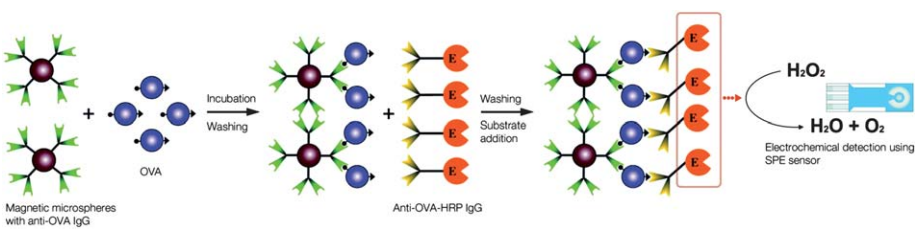

Scheme 1 System for detection of ovalbumin based on ELISA combined with electrochemical monitoring.

was kept at this temperature for 1 h. $SnCl_4$ (1.12 ml) was added and the mixture refluxed at 80 °C for 20 h. The hypercrosslinked (HPSX; X = M, E or O for chloromethylation with CMME, CMEE or CMOE, respectively) microspheres were then kept in anhydrous DCE for 12 h, filtered and washed successively with 1,2-dichloroethane, ethanol and diethyl ether before vacuum drying at 40 °C.

Sulfonation of HPSX microspheres. HPSX (X = M, E or O for chloromethylation with CMME, CMEE or CMOE, respectively) microspheres (1 g) were placed in a 50 ml round-bottomed flask, swollen in DCE (16 ml) for 10 h, 96% H_2SO_4 (4 g) and Ag_2SO_4 (12.5 mg) were added and the mixture was refluxed at 80 °C for 2 h. After completing the sulfonation, the microspheres (denoted as HPSX-SO_3^-) were washed five times with 0.2 M H_2SO_4 and water and vacuum-dried at 40 °C for 24 h. The content of SO_3^- groups was determined by sulfur analysis.

Precipitation of iron oxide in HPSX-SO_3^- microspheres. HPSX-SO_3^- microspheres were charged in a 100 ml round-bottomed reaction vessel equipped with an anchor-type stirrer (150 rpm). The microspheres (1 g) were dispersed in water (40 ml) at room temperature for 4 h. Subsequently, $FeCl_3 \cdot 6H_2O$ and $FeCl_2 \cdot 4H_2O$ (the amounts are given in Table 1) were dissolved in the above-mentioned suspension ($FeCl_3/FeCl_2$ = 2/1 mol/mol), which was then evacuated (2.7 kPa) at 23 °C for 1 h. Vacuum was removed and the reaction mixture was heated up to 80 °C. 25% aqueous ammonia (50% excess) was then dropwise added and the mixture refluxed for 30 min. After completing the reaction, the mixture was cooled to room temperature. The resulting magnetic (HPSX-M-SO_3^-) microspheres were separated using a magnet, ten times washed with water and finally vacuum dried at 40 °C for 24 h.

Immobilization of HRP on HPSM-M4-SO_3^- microspheres and determination of enzyme activity. HPSM-M4-SO_3^- microspheres (1 mg, 29 μl of suspension with a concentration of 35 mg particles per ml) were washed five times with 0.1 M phosphate buffer (pH 7.3). HRP (3 mg) in 0.1 M phosphate buffer (1 ml) was added and the mixture incubated at 4 °C for 16 h under mild shaking. After completion of the immobilization, the resulting HRP-HPSM-M4-SO_3^- microspheres were washed eight times with phosphate buffer.

The activity of immobilized enzyme was determined using hydrogen peroxide as a substrate and 1,2-phenylenediamine (OPD) as a chromogen according to an earlier published method.[45] A solution of the substrate was prepared from 0.1 M phosphate buffer (20 ml, pH 6.2), 30% hydrogen peroxide (10 μl) and OPD (10 mg). The solution (100 μl) was added to the suspension of HRP-HPSM-M4-SO_3^- microspheres (100 μl) and after incubation at 37 °C for 10 min under mild shaking UV absorbance of the supernatant was measured at 492 nm.

Direct immobilization of primary antibodies (anti-OVA IgG) on HPSM-M4-SO_3^- microspheres. HPSM-M4-SO_3^- microspheres (1 mg, 29 μl of suspension with concentration 35 mg ml^{-1}) were washed five times with 0.1 M MES buffer (pH 5) and a solution of anti-OVA IgG (100 μg) in MES buffer (500 μl) was added. The immobilization proceeded at 4 °C for 16 h under mild shaking. The anti-OVA-HPSM-M4-SO_3^- microspheres were washed five times with MES buffer, non-specifically adsorbed antibodies were removed after incubation with 0.05% trifluoroacetic acid (TFA; 2 × 200 μl) at 23 °C for 5 min. Finally, the microspheres were washed five times with 0.1 M MES buffer.

The immobilization efficiency was estimated by SDS-PAGE in Tris/glycine according to the following procedure. Electrophoresis was performed on a linear 12% SDS–polyacrylamide gel of 0.75 mm thickness. The samples were mixed with Laemmli buffer (1 : 1 v/v) and boiled at 100 °C for 2 min. SDS-PAGE proceeded in a Mini-PROTEAN electrophoresis cell (Bio-Rad, Philadelphia, USA) at 180 V with Tris/glycine/SDS running buffer (25 mM Tris, 192 mM glycine, 0.1 wt% SDS). Gels were stained by a conventional silver staining method.

Affinity isolation of ovalbumin and electrochemical detection. A solution of antigen ovalbumin (OVA) in 0.1 M phosphate buffer (500 μl; pH 7) was added to the suspension of anti-OVA-HPSM-M4-SO_3^- microspheres (OVA : anti-OVA 2 : 1 mol/mol) and the mixture was incubated at 23 °C for 45 min under mild shaking. The microspheres were then washed with 0.1 M phosphate buffer (pH 7), 0.1 M phosphate buffer (pH 7) containing 1 M NaCl and 0.1 M phosphate buffer (pH 7), three times each. To detect specifically bound OVA, the secondary antibody (anti-OVA-HRP conjugate) diluted 1 : 20 000 with 0.1 M hydrogencarbonate buffer (pH 9.49) containing 0.1% BSA and 0.05% Tween 20 was added. The reaction proceeded at 37 °C for 45 min under gentle shaking. Finally, to electrochemically monitor the signal decrease of substrate due to enzymatic reaction of conjugate label and substrate, unbound conjugate was removed by washing five times with 0.1 M phosphate buffer. Hydrogen peroxide (800 μl; 15 mg l^{-1}) was added for final electrochemical measurement depending on the above mentioned conditions. HPSM-M4-SO_3^- microspheres were used as a control.

Electrochemical linear sweep voltammetry (LSV) measurement. All electrochemical measurements were performed on a PalmSens

Table 1 Preparation of HPSX-M-SO_3^- microspheres containing γ-Fe_2O_3; Fe(III)/Fe(II) = 2/1 (mol/mol)

Microspheres	Fe(II) + Fe(III) salts[a] (wt%)	Fe (wt%) in microspheres		
		CA[b]	AAS[c]	TGA[d]
HPSM-M1-SO_3^-	2.2	26	23	45
HPSM-M2-SO_3^-	3.4	35	33	25
HPSM-M3-SO_3^-	5.6	46	41	31
HPSM-M4-SO_3^-	6.8	54	53	52
HPSM-M5-SO_3^-	8.0	55	53	46
HPSE-M1-SO_3^-	2.2	23	16	16
HPSE-M2-SO_3^-	3.4	24	17	15
HPSE-M3-SO_3^-	5.6	44	40	38
HPSE-M4-SO_3^-	6.8	37	32	31
HPSE-M5-SO_3^-	8.0	40	38	35
HPSO-M1-SO_3^-	2.2	26	23	23
HPSO-M2-SO_3^-	3.4	36	37	34
HPSO-M3-SO_3^-	5.6	45	46	39
HPSO-M4-SO_3^-	6.8	45	45	41
HPSO-M5-SO_3^-	8.0	44	44	42

[a] Content of ferrous and ferric chlorides in reaction mixture. [b] By carbon analysis. [c] By AAS. [d] By TGA.

compact electrochemical sensor interface (Palm Instruments BV; Houten, Netherlands). Screen-printed three-electrode sensors (SPEs) comprised reference Ag/AgCl electrode, platinum working and auxiliary electrodes (type AC1.W2.R1, BVT Technologies, Brno, Czech Republic) for sensing substrate hydrogen peroxide after its enzymatic conversion by HRP. 0.1 M phosphate buffer (pH 7.3) containing 0.15 M NaCl was used in all assays. Measurement conditions were the following: potential range 0–1 V with 0.005 V steps, scan rate 0.1 V s^{-1}, equilibration time 2 s. The current value at the potential 0.5 V was read-out for evaluation of results.

Characterization

The microspheres were observed in an Opton III light microscope (Oberkochen, Germany) and photographed using a Canon EOS 400D camera (Tokyo, Japan). The microsphere size in the dry state and their size distribution were analyzed by scanning electron microscopy (SEM; JEOL JSM 6400; TEM Tecnai Spirit G2, FEI, Brno, Czech Republic) and the number-average diameter (D_n), weight-average diameter (D_w) and uniformity (D_w/D_n) were calculated using an Atlas software (Tescan Digital Microscopy Imaging, Brno, Czech Republic) by counting at least 500 individual microspheres on SEM micrographs. The D_n and D_w can be expressed as follows:

$$D_n = \sum n_i D_i / \sum n_i \quad (1)$$

$$D_w = \sum n_i D_i^4 / \sum n_i D_i^3 \quad (2)$$

where n_i and D_i are the number and diameter of the i^{th} microsphere, respectively.

S_{BET} of microspheres was determined by nitrogen adsorption in liquid nitrogen (77 K) using a Gemini VII 2390 Analyzer (Micromeritics, Norcross, USA).

The specific pore volumes and the pore size distribution of dry microspheres were determined with a Pascal 140 and 440 mercury porosimeter (Thermo Finigan, Rodano, Italy) in two pressure intervals, 0–400 kPa and 1–400 MPa, allowing evaluation of meso- and macropores. Because macropores are not pertinent in this study, only the volume and size of mesopores were considered. The pore volume and the most frequent mesopore diameter were calculated from the cumulative pore volume curves assuming a cylindrical pore model by the Pascal program using Washburn's equation describing capillary flow in porous materials.[46]

The microspheres were analyzed using a Perkin Elmer 2400 Series CHNS/O elemental analyzer (Shelton, CN, USA). The absorbance was measured with a Biochrom Libra S22 UV/VIS spectrophotometer (Cambridge, UK). The content of Fe was analyzed by atomic absorption spectroscopy (AAS). The relative content of polystyrene and iron oxide was determined using a Perkin Elmer TGA 7 Thermogravimetric Analyzer (Norwalk, CT, USA). The magnetic microspheres were heated from room temperature to 860 °C at a heating rate of 10 °C min^{-1} in air, allowing the polymer to completely decompose while the inorganic iron oxides were determined as the residue.

Magnetic measurements. Magnetization curves were measured at room temperature using an EV9 vibrating magnetometer (DSM Magnetics, ADE Corporation, Lowell, MA, USA) with the maximum magnetic field of 2 T. The temperature dependence of magnetic susceptibility, κ, was measured from liquid nitrogen temperature (77 K) to *ca.* 1000 K using a KLY-4S/CS-3 kappabridge (AGICO Brno, Czech Republic) according to a previously described procedure.[47] The measurements were carried out in ambient atmosphere; the heating rate was 8.5 K min^{-1}.

Results and discussion

Dispersion copolymerization of styrene and divinylbenzene

Dispersion polymerization is a convenient single-step technique for preparation of monodisperse micrometre-sized particles. Here, PS microspheres with size ranging from 2.5 to 5.2 μm were prepared by dispersion copolymerization of S and DVB in a MetCel/EtOH mixture. The dispersion was stabilized with (2-hydroxypropyl)cellulose and the polymerization was initiated with dibenzoyl peroxide. The concentrations of the stabilizer, initiator and MetCel/EtOH ratio were kept constant throughout the experiments at 1.58 wt%, 4.4 wt% and 0.5 w/w, respectively. In order to make the microspheres insoluble in organic solvents, a small amount of DVB (1 wt%) was added to the reaction mixture for obtaining lightly crosslinked non-porous microspheres ($S_{BET} \approx 5$ m^2 g^{-1}). Because DVB in the polymerization mixture can interfere with a homogeneous nucleation mechanism resulting in wrinkled particles in an undesirable secondary nucleation,[36] continuous addition of DVB at various rates was investigated.

After addition of the whole amount of DVB five minutes after beginning of the polymerization in one portion, 5.2 μm PS microspheres with a very broad size distribution ($D_w/D_n = 1.91$; Fig. 1a) were obtained. One of the reasons for formation of polydisperse particles may be ascribed to different reactivity ratios for DVB isomers and S. As *p*-DVB has a higher reactivity ratio ($r_2 = 1.18$) than S ($r_1 = 0.26$),[48] *p*-DVB is capable of formation of new nuclei broadening thus the distribution. Polydispersity may be also caused by slow initiation of the system.[49]

When DVB was added continuously, at a rate of 2 μl every 30 s for 30 min, the primary particles aggregated in 2.5 μm cauliflower-like structures (Fig. 1b). The aggregation could be caused by very fast addition of DVB which was not completely accommodated in polymer–monomer particles. As a result, new particles were attached to the primary ones forming cauliflower morphology. If DVB was continuously added at a rate of 2 μl every 45 s for 45 min, PS microspheres had an average size of 3.7 μm and $D_w/D_n = 1.16$ (Fig. 1c). The microspheres were almost monodisperse; it could be thus assumed that this mode of DVB addition was appropriate for preparation of the particles. Such microspheres were tested for immobilization of anti-OVA and subsequent detection of OVA. *Ca.* 4.5 μm PS microspheres ($D_w/D_n = 1.34$) were obtained at a dosing rate of 2 μl DVB every 60 s in the course of 60 min (Fig. 1d). The presence of small amounts of tiny (0.7 μm) particles among larger microspheres indicated that the nucleation was not fast enough. Finally, DVB was continuously added at a rate of 2 μl every 75 s for 75 min and 4.8 μm PS microspheres of a rather narrow size distribution ($D_w/D_n = 1.17$) were obtained (Fig. 1e). It could be thus stated

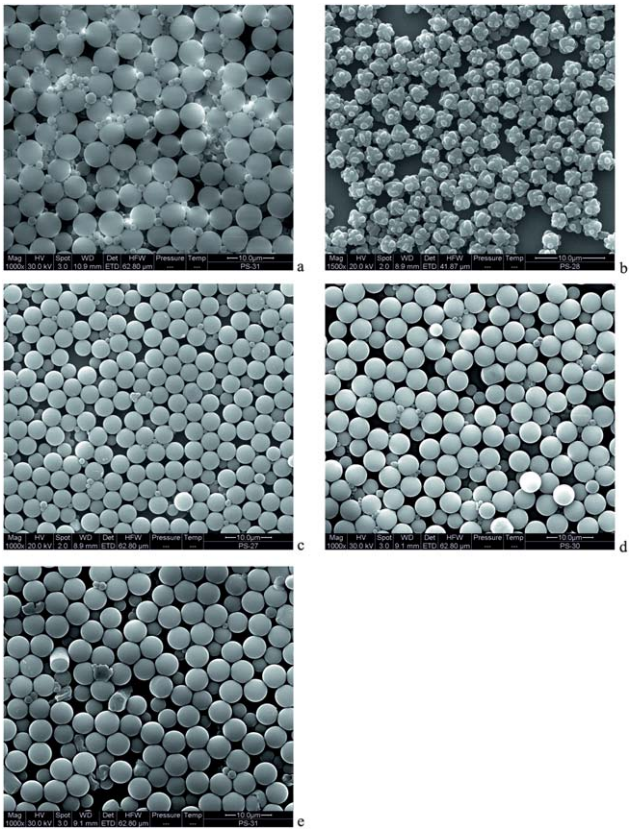

Fig. 1 SEM micrographs of (a–e) PS microspheres prepared by dispersion polymerization of styrene and DVB in 2-methoxyethanol/ethanol mixture. DVB was added 5 min after starting of the polymerization: (a) 0.11 g (120 μl) in one portion, (b) 2 μl every 30 s for 30 min, (c) 2 μl every 45 s for 45 min, (d) 2 μl every 60 s for 60 min and (e) 2 μl every 75 s for 75 min. The polymerization was stabilized by 1.58 wt% HPC.

that the particle size increased with prolonging time of DVB addition. The result could be explained by decreasing *in situ* DVB concentration with increasing rate of DVB addition which is in agreement with literature data.[50] Moreover, the narrowing of the particle size distribution could be ascribed to a decrease in solubility of polymer chains in the medium with increasing concentration of DVB in the reaction mixture leading to the formation of more nuclei. However, their size was smaller.[51]

Hypercrosslinking of PS microspheres and sulfonation of HPSX microspheres

With the aim to efficiently modify benzene rings of PS and subsequently produce large S_{BET} in the microspheres, three chloromethylated ethers were investigated. PS microspheres were chloromethylated with CMME, CMEE or CMOE in DCE and hypercrosslinked using the $SnCl_4$ catalyst. The resulting HPSX microspheres had large S_{BET} ranging from 367 to 1212 $m^2\ g^{-1}$ as determined by BET isotherm obtained by adsorption of nitrogen. Some of them, however, partly aggregated. Hypercrosslinked CMME-chloromethylated polystyrene microspheres (HPSM) had the largest S_{BET} = 1212 $m^2\ g^{-1}$. This could be ascribed to the fact that small CMME molecule easily penetrated into the swollen PS network. CMME was the most reactive of all the investigated chloromethylation agents. Due to its highly efficient Friedel–Crafts alkylation (0.65 mmol Cl g^{-1}), many chloromethyl groups were introduced bridging the benzene rings of PS microspheres. Fine porous structure of HPSM microspheres with pore size in the range of tens of nanometres was confirmed by a TEM micrograph of the cross-section (Fig. 2a). Every HPSX microsphere consisted of *ca.* 10 nm PS globules between which *ca.* 10–40 nm pores were formed.

Hypercrosslinking of CMEE-chloromethylated microspheres (HPSE) produced somewhat lower, but still sufficient, S_{BET} = 929 $m^2\ g^{-1}$. Also CMEE molecule was small enough and its access into the network was easy to chloromethylate PS microspheres (0.55 mmol Cl per g). The smallest S_{BET} = 367 $m^2\ g^{-1}$ was achieved with microspheres obtained by hypercrosslinking CMOE-chloromethylated particles (HPSO). The CMOE reagent was obviously not as reactive as CMME and CMEE providing insufficient amounts of chloromethyl groups (0.27 mmol Cl per g).

Determination of micro/mesoporous structure of hypercrosslinked HPS microspheres by nitrogen adsorption was completed by characterization of mesoporous structure by mercury porosimetry measurements. Macroporosity was not considered due to a small size of the microspheres. The most frequent pore radius of HPSM microspheres was mostly in the range 8–24 nm (Fig. 3), the cumulative pore volume was 0.4 ml g^{-1} and the mesoporosity amounted to 29%. Porous properties of the HPSO microspheres resembled those of HPSM particles. The most frequent pore radius was 6–20 nm, the cumulative pore volume 0.3 ml g^{-1} and mesoporosity 23%. Compared with HPSM and HPSO microspheres, mesoporosity of the HPSE microspheres was higher (34%). Their most frequent pore radius was also larger ranging from 7 nm to 25 nm, which was accompanied by a high cumulative pore volume of 0.43 ml g^{-1}.

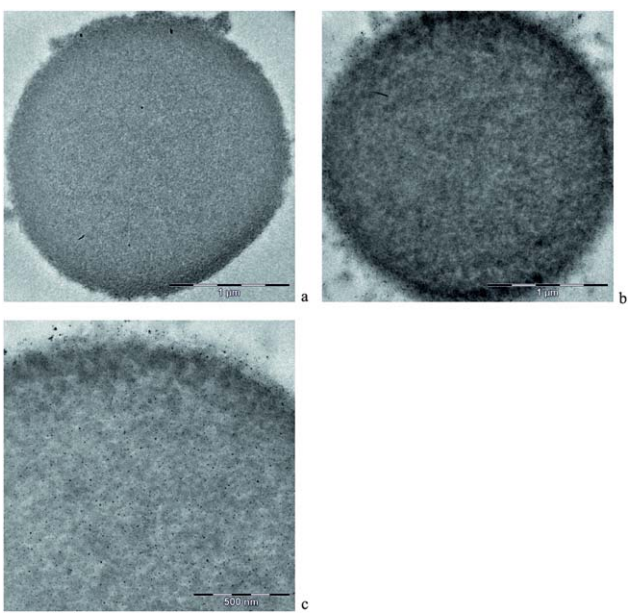

Fig. 2 TEM micrographs of cross-sections of (a) HPSM and (b and c) HPSM-M5-SO_3^- microspheres. Magnification 37 000× (a and b) and 59 000× (c).

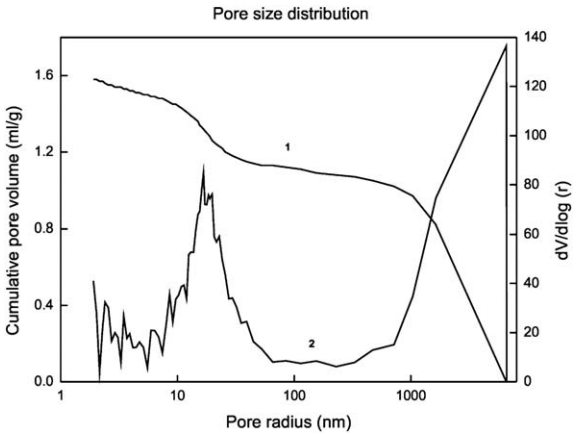

Fig. 3 (1) Cumulative pore volume V and (2) pore size distribution $dV/d\log(r)$ curves of CMME-hypercrosslinked HPSM (1 wt% DVB) microspheres determined by mercury porosimetry; pore radii range 1.9 nm–10 μm (mesopore radii analyzed up to 25 nm).

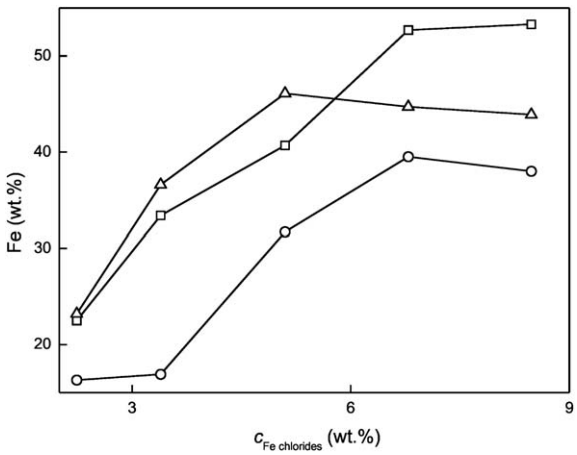

Fig. 4 Dependence of Fe content (by AAS) in HPSX-SO3$^-$ microspheres on $FeCl_x$ concentration c in the reaction mixture. Chloromethylation with (□) CMME, (○) CMEE and (△) CMOE.

Functionalization of microsphere surface is necessary to make coupling of antibody (anti-ovalbumin) on the surface by covalent bonds possible. In this report, sulfonation was selected for modification of hypercrosslinked PS microspheres because it is an easy and reliable reaction. Silver sulfate-catalyzed reaction of 96% sulfuric acid yielded HPSX-SO_3^- microspheres containing *ca.* 4 mmol SO_3^- per g according to sulfur analysis.

Precipitation of iron oxide within HPSX-SO_3^- microspheres

Fe(II) and Fe(III) salts were precipitated in the pores of the HPSX-SO_3^- microspheres by alkaline medium performed by Massart's procedure.[52] Ferrous and ferric chloride solutions were first imbibed in the porous structure in vacuum and precipitation was achieved by aqueous ammonia. Although the concentration of ferrous and ferric chlorides in the aqueous phase was varied from 2 to 8.5 wt%, the Fe^{2+}/Fe^{3+} ratio was kept constant (2/1 mol/mol).

Successful embedding of iron oxide in the PS matrix was documented by TEM of cross-sections in HPSM-M5-SO_3^- microspheres (Fig. 2b and c as an example). Both non-magnetic HPSM and magnetic HPSM microspheres are composed of globules (dark spots in Fig. 2a–c) between which the pores (light spots) appear. Iron oxides in the pores can be observed as black dots (Fig. 2b and c); their size is around 9 nm, which is comparable with the pore size. This finding favors retention of the iron oxide nanoparticles inside the porous structure. However, iron oxide was precipitated also on the particle surface. As expected, filing of the pores with iron oxide nanoparticles led to a significant decrease of specific surface area. For example, S_{BET} of HPSM-M1, HPSE-M1 and HPSO-M1 microspheres decreased to 62, 58 and 20 $m^2\ g^{-1}$, respectively.

Fig. 4 shows the dependence of the iron content determined by AAS in the 3.7 μm HPSX-M-SO_3^- microspheres on the concentration of iron salts in the reaction mixture. As expected, with an increasing concentration of ferrous and ferric chlorides in the reaction mixture, the content of Fe precipitated in the microspheres increased reaching a plateau at high iron chloride concentration (5.1 wt% for HPSO-M3-SO_3^- and 6.8 wt% for HPSM-M4-SO_3^- and HPSE-M4-SO_3^-). This could be explained by washing out of iron oxides from the microspheres at higher iron salt concentrations. It can be assumed that the precipitated iron oxide was in the form of maghemite (γ-Fe_2O_3) due to the presence of oxygen in the aqueous medium which oxidized the primarily formed Fe_3O_4. The amount of iron in the microspheres was determined not only by AAS but by elemental analysis and thermogravimetric analysis (TGA) as well. Elemental analysis, in particular the percentage of carbon, can be used for calculating the percentage of γ-Fe_2O_3 in HPSX-M-SO_3^- microspheres since the original neat PS microspheres do not contain Fe. The following equation was used:

$$\%(\gamma\text{-}Fe_2O_3) = 100 - \text{PS}\ (\%) = 100 - [\text{C}\ (\%)/89.8)] \times 100, \quad (3)$$

where % of C was obtained from elemental analysis of HPS-M-SO_3^- microspheres and 89.8 was the content of C found in neat PS microspheres. For example, the C content in HPSE-M1-SO_3^- microspheres was 61.1% and the calculated PS content in the magnetic microspheres was 68 wt%, *i.e.*, the γ-Fe_2O_3 content was 32 wt% which corresponds to 23.1 wt% Fe (Table 1). The contents of Fe determined by elemental analysis were in rough agreement with those obtained by AAS (Table 1). The iron content determined in the microspheres by the above mentioned three methods decreased in the order HPSM ≈ HPSO > HPSE (Table 1).

TGA of HPSX-M-SO_3^- microspheres was measured at temperatures ranging from 40 to 860 °C. As an example, the temperature-dependent decomposition of HPSE-M4-SO_3^- microspheres is shown in Fig. 5. A temperature increase was accompanied by a gradual mass loss. The main decomposition started at around 330 °C where the HPSE-M4-SO_3^- microspheres began to rapidly lose weight with the mass loss around 50% up to 420 °C (Fig. 5). In the degradation of polystyrene, random main-chain scission occurs below 300 °C, where the weak links play a significant role.[53] At temperatures above 300 °C, volatile products are formed, containing monomers (45%) and oligomers. The value 125.5 kJ mol^{-1} was determined by DSC for the activation energy of polystyrene degradation[53]

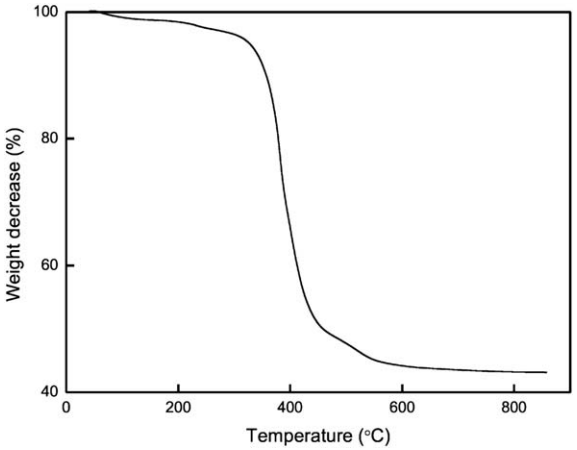

Fig. 5 Thermogravimetric analysis of HPSE-M4-SO_3^- microspheres.

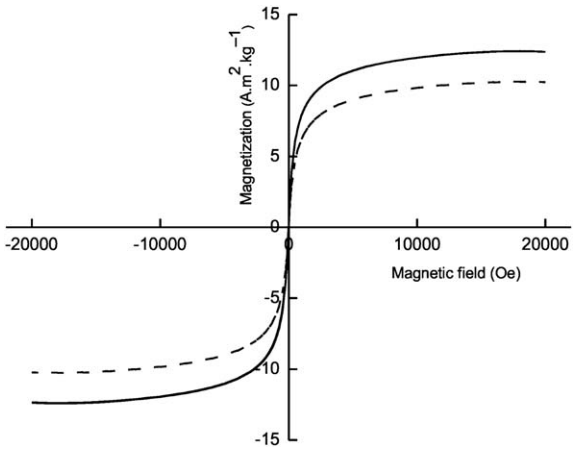

Fig. 6 Induced magnetization of HPSM-M5-SO_3^- (full line) and HPSE-M5-SO_3^- (dashed line) microspheres.

and this value was found to be independent of the atmosphere in which the degradation took place (air, nitrogen or oxygen). At the end of the TGA analysis performed in air, the organic phase of HPSE-M4-SO_3^- microspheres was completely decomposed around 600 °C, allowing one to calculate the iron oxide content as the inorganic residue. The determination of iron in magnetic microspheres by the three methods was mostly in agreement. Generally, the content of precipitated iron oxide increased with increasing concentration of Fe salts in the feed. However, some differences between the results, obtained from TGA, AAS or elemental analysis, were observed, *e.g.*, in HPSM-M1-SO_3^- microspheres where the Fe content as determined by TGA was higher compared with the other two methods. This might be due to inaccurate results of TGA of microspheres containing low amounts of precipitated iron oxides. The data scattering in Table 1 could be explained by a release of iron oxide captured on the particle surface during washing. HPSM-M4-SO_3^- microspheres contained the highest amount of iron ($\sim$ 53 wt%).

Magnetic properties

The induced magnetization curves of HPSM-M5-SO_3^- and HPSE-M5-SO_3^- microspheres at room temperature are shown in Fig. 6. Negligible hysteresis in the magnetization curves suggests a significant superparamagnetic contribution of the iron oxide precipitated inside the hypercrosslinked microsphere pores. As expected, HPSM-M5-SO_3^- microspheres displayed higher saturation magnetization (M_s) than the HPSE-M5-SO_3^- ones. The γ-Fe_2O_3 content in the microspheres estimated from magnetic measurements (Table 2) was lower than that from the Fe contents obtained by carbon analysis (CA), AAS and TGA (Table 1). The reduced M_s values could be ascribed to various surface effects, such as oxidation resulting in low-magnetic compounds, imperfections in the crystal structure, deviation from stoichiometry and adsorbed materials.[54] It should be noted that the saturation magnetization of small particles is always lower than that of the bulk. Magnetic parameters obtained from measurements of magnetization curves included also mass-specific magnetic susceptibility χ measured at room temperature (Table 2). The value of saturation magnetization M_s, which is a direct measure of the concentration of atomic magnetic moments, was used to estimate the relative concentrations of magnetic iron oxide nanoparticles in HPSM-M5-SO_3^-, HPSE-M4-SO_3^-, HPSE-M5-SO_3^- and HPSO-M5-SO_3^- microspheres (Table 2), assuming that the reported saturation magnetization of bulk maghemite (γ-Fe_2O_3) is 84 $Am^2\ kg^{-1}$ (ref. 55) and that of pure maghemite nanoparticles is 55.9 $Am^2\ kg^{-1}$.[56]

Thermomagnetic analysis revealed analogous behavior of all analyzed magnetic microspheres. As an example, the temperature dependence of magnetic susceptibility of HPSM-M5-SO_3^- is shown in Fig. 7. A pronounced maximum of magnetic susceptibility was observed at 120 °C, followed by a sharp decrease with a local minimum between 350 °C and 450 °C and an increase with different intensity. Finally, the decrease starting at about 550–570 °C indicated the presence of magnetite, which was obviously the final product of thermal transformations. The absence of the Verwey transition around −150 °C suggested a lack of multidomain magnetic particles. The interpretation is

Table 2 Characteristics of HPSX-M-SO_3^- microspheres containing γ-Fe_2O_3

Microspheres	$\chi^a \times 10^{-4}/m^3\ kg^{-1}$	$H_c{}^b$/Oe	$M_{rs}{}^c/10^{-1}$ A $m^2\ kg^{-1}$	$M_s{}^d$/A $m^2\ kg^{-1}$	$(M_{rs}/M_s)^e \times 10^{-2}$	γ-$Fe_2O_3{}^f$ (wt%)
HPSM-M5-SO_3^-	5.17	3.78	0.592	11.80	0.501	21.2
HPSE-M4-SO_3^-	5.50	15.16	2.060	8.71	2.360	15.3
HPSE-M5-SO_3^-	4.18	4.92	0.772	9.70	0.796	17.3
HPSO-M5-SO_3^-	5.50	4.39	0.844	11.60	0.727	20.8

[a] Magnetic susceptibility. [b] Coercive force. [c] Remanent saturation magnetization. [d] Saturation magnetization. [e] Remanent saturation/saturation magnetization ratio. [f] The γ-Fe_2O_3 content in the microspheres was calculated relative to M_s of pure γ-Fe_2O_3 nanoparticles (55.9 $Am^2\ kg^{-1}$).

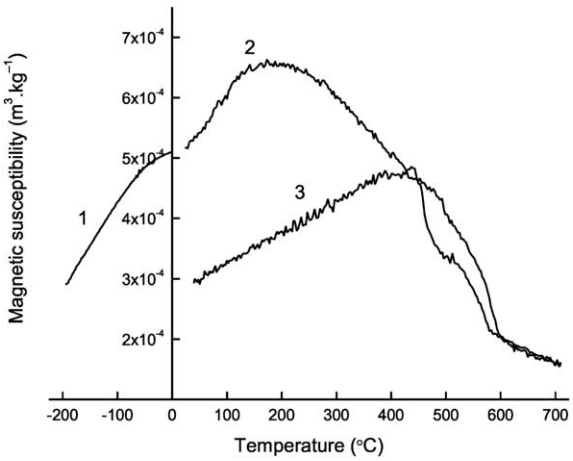

Fig. 7 Temperature dependence of magnetic susceptibility of HPSM-M5-SO_3^- microspheres. (1) Low-temperature curve, (2) heating curve and (3) cooling curve.

unclear, but this could be probably related to disintegration of microspheres and subsequent reduction of maghemite to magnetite.

Direct immobilization of HRP and anti-OVA on HPSM-M4-SO_3^- microspheres

As a model system for construction of immunomagnetic biosensor for sandwich ELISA-based protein detection, primary antibody (anti-OVA)/antigen (OVA)/secondary antibody (anti-OVA-HRP) was selected. Anti-OVA was therefore immobilized on HPSM-M4-SO_3^- microspheres. The immobilization efficiency investigated by the standard Tris/glycine SDS-PAGE[57] with silver staining[58] was higher than 90% (Fig. 8).

In lane 1, there was pure anti-OVA as a positive control. The supernatant after immobilization was in lane 2. This lane was compared with the first lane and it was concluded that almost all anti-OVA was immobilized on HPSM-M4-SO_3^- microspheres. The first and second eluents were in lanes 3 and 4, respectively. Blind runs confirmed that anti-OVA was not released from HPSM-M4-SO_3^- microspheres after immobilization.

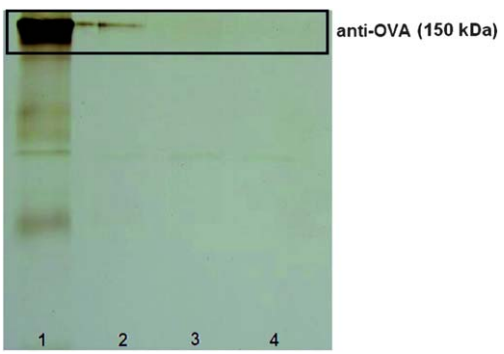

Fig. 8 Tris/glycine SDS-PAGE of anti-OVA antibodies immobilized onto M-PS-SO_3H microspheres. Original anti-OVA IgG (lane 1), supernatant after immobilization (lane 2), first (lane 3) and second washing after immobilization (lane 4).

Electrochemical measurements

The reaction between antigen and antibody proceeds generally on the surface of the working electrode, where the limiting factors are regeneration of the sensor and reusability.[59] The problems can be avoided by using magnetic microspheres with immobilized antibodies enabling us to perform immunoreactions separately from electrochemical detection.

From a variety of tested sweep and pulse electrochemical techniques, linear sweep voltammetry (LSV) was found to be the most suitable for hydrogen peroxide detection (Fig. 9). The conditions of electrochemical measurements, such as potential range, steps, equilibration time and scan rate, with SPEs were optimized using HRP-HPSM-M4-SO_3^- microspheres. The advantage of HRP-HPSM-M4-SO_3^- microspheres is the incorporation of superparamagnetic iron oxide cores within PS particles. Substrate is then protected from the contact with iron oxide suppressing thus possible electrocatalytic oxidation of hydrogen peroxide.

Finally, affinity isolation of ovalbumin was performed and electrochemically detected after recognition of the specific secondary antibodies (conjugate) of the formed immunocomplex. A complete immunomagnetic biosensor for electrochemical determination of protein (OVA) based on sandwich ELISA was constructed using a model system primary antibody (anti-OVA)/antigen (OVA)/secondary antibody (anti-OVA-HRP). Anti-OVA IgG was immobilized on HPSM-M4-SO_3^- microspheres and used for affinity isolation of OVA antigen at the anti-OVA/OVA ratio 1 : 2 (mol/mol). To confirm the affinity OVA isolation, the HRP-labeled secondary antibody (anti-OVA-HRP) diluted 1 : 20 000 was added. Hydrogen peroxide (substrate) was then used to verify the immunocomplex formation and the corresponding current decrease was electrochemically monitored (Fig. 10). Anti-OVA-HPSM-M4-SO_3^-/OVA/anti-OVA-HRP microspheres were compared with HPSM-M4-SO_3^- microspheres (as control) to validate the system functionality. The current decrease in time induced by oxidation of hydrogen peroxide with the HRP-labeled conjugate proved that HPSM-M4-SO_3^- microspheres are suitable for combination of

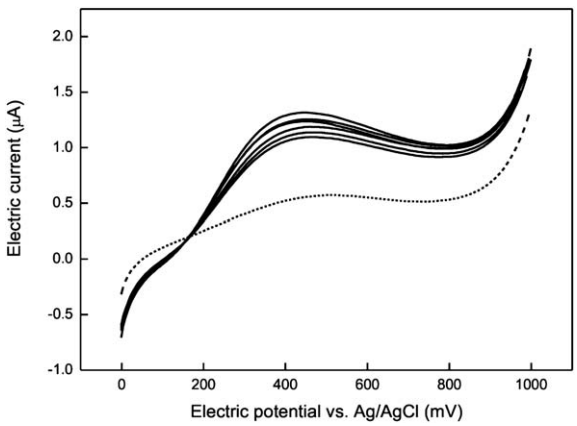

Fig. 9 Electric current change induced by the conversion of hydrogen peroxide by HRP-HPSM-M4-SO_3^- microspheres. Medium: 0.1 M phosphate buffer (pH 7) containing 0.15 M NaCl and hydrogen peroxide (substrate; 20 mg l^{-1}).

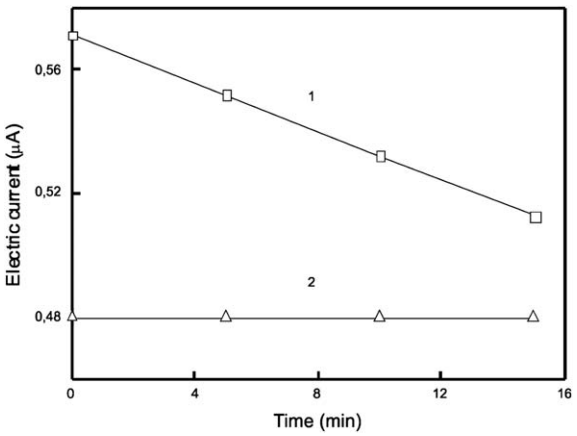

Fig. 10 Electrochemical detection of H_2O_2 consumption using anti-OVA-HPSM-M4-SO_3^-/OVA/anti-OVA-HRP microspheres (curve 1). HPSM-M4-SO_3^- microspheres served as a control (curve 2). Medium: 0.1 M phosphate buffer (pH 7) containing 0.15 M NaCl; anti-OVA/OVA 1/2 (mol/mol), conjugate dilution 1 : 20 000, 15 mg of H_2O_2 per l.

ELISA-based protein detection with a highly sensitive electrochemical determination. At present, OVA detection was only qualitative; quantitative determination is in progress.

Conclusions

Homogeneous (non-porous) PS microspheres with a rather narrow size distribution were prepared by controlled polymerization of styrene with small amounts of divinylbenzene (1 wt%) as a crosslinking agent. Porous structure was then formed by hypercrosslinking of chloromethylated PS microspheres providing sufficiently large space for precipitation of iron oxides. Subsequent hypercrosslinking was, however, accompanied by partial aggregation of the microspheres. In the next steps, the microspheres were sulfonated with sulfuric acid and iron oxide subsequently incorporated into pores of the sulfonated hypercrosslinked microspheres by precipitation of Fe(II)/Fe(III) salts. As far as we know, this is the first example of preparation of strongly magnetic supports by taking advantage of highly microporous structure of hypercrosslinked microspheres. As the sulfo groups enable immobilization of biomolecules, an anti-OVA antibody was attached to the surface of the magnetic microspheres without adversely influencing the functions of immobilized ligands, *e.g.*, enzyme activity and capability of antibodies of affinity interactions. The specific model system served for construction of an electrochemical immunosensor for detection of ovalbumin protein, which can be easily assayed using linear sweep voltammetry with a three-electrode screen-printed sensor with platinum working electrode. Systems based on electrochemical monitoring of proteins are promising, *e.g.*, for detection of biomarkers specific to various diseases.

Acknowledgements

The financial support of the European Union (grants CaMiNEMS no. 228980 and NaDiNe no. 246513), Grant Agency of the Czech Republic (grants 203/09/0857 and 203/09/1242) and Ministry of Education, Youth and Sports (grants 0021627502 and LC06035) is gratefully acknowledged.

References

1 B. Hickstein and U. A. Peuker, *Biotechnol. Prog.*, 2008, **24**, 409.
2 M. Slováková, J. M. Peyrin, Z. Bílková, M. Jukličková, L. Hernychová and J. L. Viovy, *Bioconjugate Chem.*, 2008, **19**, 966.
3 R. Handgretinger, P. Lang, M. Schumm, G. Taylor, W. Schwinger, E. Koscielniak, A. Reiter, C. Peters, D. Niethammer and T. Klingebiel, *Bone Marrow Transplant.*, 1998, **21**, 987.
4 B. Rittich, A. Španová, D. Horák, M. J. Beneš, L. Klesnilová, K. Petrová and A. Rybníkář, *Colloids Surf., B*, 2006, **52**, 143.
5 Z. C. Zhang, L. M. Zhang, L. Chen, L. G. Chen and Q. H. Wan, *Biotechnol. Prog.*, 2006, **22**, 514.
6 M. Franzreb, M. Siemann-Herzberg, T. J. Hobley and O. R. T. Thomas, *Appl. Microbiol. Biotechnol.*, 2006, **70**, 505.
7 R. P. Liu, J. T. Liu, L. Xie, M. X. Wang, J. P. Luo and X. X. Cai, *Talanta*, 2010, **81**, 1016.
8 B. Rittich, A. Španová, P. Šálek, P. Němcová, Š. Trachtová and D. Horák, *J. Magn. Magn. Mater.*, 2009, **321**, 1667.
9 J. R. Whiteaker, L. Zhao, H. Y. Zhang, L. C. Feng, B. D. Piening, L. Anderson and A. G. Paulovich, *Anal. Biochem.*, 2007, **362**, 44.
10 J. F. Peter and A. M. Otto, *Proteomics*, 2010, **10**, 628.
11 P. B. Luppa, L. J. Sokoll and D. W. Chan, *Clin. Chim. Acta*, 2001, **314**, 1.
12 S. Centi, S. Laschi and M. Mascini, *Talanta*, 2007, **73**, 394.
13 W. Liang, W. Yi, Y. Li, Z. Zhang, M. Yang, C. Hu and A. Chen, *Mater. Lett.*, 2010, **64**, 2616.
14 O. D. Renedo, M. A. Alonso-Lomillo and M. J. A. Martínez, *Talanta*, 2007, **73**, 202.
15 F. H. Chen, Q. Gao, G. Y. Hong and J. Z. Ni, *J. Magn. Magn. Mater.*, 2008, **320**, 1921.
16 Y. Zhou, S. X. Wang, B. J. Ding and Z. M. Yang, *Chem. Eng. J.*, 2007, **138**, 578.
17 Y. B. Sun, X. B. Ding, Z. H. Zheng, X. Cheng, X. H. Hu and Y. X. Peng, *Eur. Polym. J.*, 2007, **43**, 762.
18 H. X. Liu, C. Y. Wang, Q. X. Gao, X. X. Liu and Z. Tong, *Acta Biomater.*, 2010, **6**, 275.
19 D. Horák and N. Benedyk, *J. Polym. Sci., Part A: Polym. Chem.*, 2004, **42**, 5827.
20 C. Oh, Y. G. Lee, C. U. Jon and S. G. Oh, *Colloids Surf., A*, 2009, **337**, 208.
21 Y. Mori and H. Kawaguchi, *Colloids Surf., B*, 2007, **56**, 246.
22 J. S. Nunes, C. L. de Vasconcelos, F. A. O. Cabral, J. H. de Araujo, M. R. Pereira and J. L. C. Fonseca, *Polymer*, 2006, **47**, 7646.
23 S. Lu, J. Ramos and J. Forcada, *Langmuir*, 2007, **23**, 12893.
24 M. Slováková, J.-M. Peyrin, Z. Bílková, M. Juklíčková, L. Hernychová and J.-L. Viovy, *Bioconjugate Chem.*, 2008, **19**, 966.
25 B. Jankovicova, S. Rosnerova, M. Slovakova, Z. Zverinova, M. Hubalek, M. Hernychova, M. Rehulka, J.-L. Viovy and Z. Bilkova, *J. Chromatogr., A*, 2008, **1206**, 64.
26 Z. Bílková, M. Slováková, N. Minc, C. Fütterer, R. Cecal, D. Horák, M. J. Beneš, I. le Potier, J. Křenková, M. Przybylski and J.-L. Viovy, *Electrophoresis*, 2006, **27**, 1811.
27 B. Hickstein and U. A. Peuker, *Biotechnol. Prog.*, 2008, **24**, 409.
28 S. S. Sun, G. L. Yang, T. Wang, Q. Z. Wang, C. Chen and Z. Li, *Anal. Bioanal. Chem.*, 2010, **396**, 3071.
29 D. Horák, M. Babič, H. Macková and M. J. Beneš, *J. Sep. Sci.*, 2007, **30**, 1751.
30 S. S. Pappel, *US Pat.*, 3 215 572, Washington, 1965.
31 R. Massart, *C. R. Acad. Sci., Ser. III*, 1980, **291**, 1.
32 M. Gonzales and K. M. Krishnan, *J. Magn. Magn. Mater.*, 2005, **293**, 265.
33 C. K. Ober, K. P. Lok and M. L. Hair, *J. Polym. Sci.*, 1985, **23**, 103.
34 C. M. Tseng, Y. Y. Lu, M. S. El-Aasser and J. W. Vanderhoff, *J. Polym. Sci., Part A: Polym. Chem.*, 1986, **24**, 2995.
35 J. Choi, S. Y. Klak, S. Kang, S. S. Lee, M. Park, S. Lim, J. Kim, C. R. Choe and S. I. Homg, *J. Polym. Sci., Part A: Polym. Chem.*, 2002, **40**, 4368.
36 B. Thomson, A. Rudin and G. Lajoie, *J. Appl. Polym. Sci.*, 1996, **59**, 2009.
37 J. Ugelstad, T. Ellingsen, A. Berge and B. Helgée, *PCT Pat.*, WO 83/03920, 1983.

38 V. A. Davankov, S. V. Rogozhin and M. P. Tsyurupa, *Vysokomol. Soedin., Ser. B*, 1973, **15**, 463.
39 N. Fontanals, P. A. G. Cormack and D. C. Sherrington, *J. Chromatogr., A*, 2008, **1215**, 21.
40 N. Fontanals, R. M. Marcé, P. A. G. Cormack, D. C. Sherrington and F. Borrull, *J. Chromatogr., A*, 2008, **1191**, 118.
41 J. Germain, J. M. J. Fréchet and F. Svec, *Small*, 2009, **5**, 1098.
42 Purolite Technical Bulletin, in *Hypersol-Macronet Sorbent Resins*, Purolite Int Ltd, UK, 1999.
43 V. A. Davankov and M. P. Tsyurupa, *Pure Appl. Chem.*, 1989, **61**, 1881.
44 M. P. Tsyurupa and V. A. Davankov, *React. Funct. Polym.*, 2002, **53**, 193.
45 J. H. Bovaird, T. T. Ngo and H. M. Lenhoff, *Clin. Chem.*, 1982, **28**, 2423.
46 S. P. Rigby, D. Barwick, R. S. Fletcher and S. N. Riley, *Appl. Catal., A*, 2003, **238**, 303.
47 F. Hrouda, *Geophys. J. Int.*, 1994, **118**, 604.
48 J. Brandrup, E. H. Immergut and E. A. Grulke, in *Polymer Handbook*, John Wiley, New York, 4th edn, 1999.
49 D. Horák, F. Švec and J. M. J. Fréchet, *J. Polym. Sci., Polym. Chem. Ed.*, 1995, **33**, 2961.
50 J. S. Song, F. Tronc and M. A. Winnik, *J. Am. Chem. Soc.*, 2004, **126**, 6562.
51 H. T. Zhang, J. X. Huang and B. B. Jiang, *J. Appl. Polym. Sci.*, 2002, **85**, 2230.
52 R. Massart, *IEEE Trans. Magn.*, 1981, **17**, 1247.
53 E. A. Turi, in *Thermal Characterization of Polymeric Materials*, Academic Press, San Diego, 2nd edn, 1981, vol. 1, p. 692.
54 F. Vereda, J. de Vicente, M. del Perto Morales, F. Rull and R. Hidalgo-Ivarez, *J. Phys. Chem. C*, 2008, **112**, 5843.
55 K. Kluchova, R. Zboril, J. Tucek, M. Pecova, L. Zajoncova, I. Safarik, M. Mashlan, I. Markova, D. Jancik, M. Sebela, H. Bartonkova, V. Bellesi, P. Novak and D. Petridis, *Biomaterials*, 2009, **30**, 2855.
56 E. Pollert, K. Knížek, M. Maryško, K. Závěta, A. Lančok, J. Boháček, D. Horák and M. Babič, *J. Magn. Magn. Mater.*, 2006, **306**, 241.
57 U. K. Laemmli, *Nature*, 1970, **227**, 680.
58 B. R. Oakley, D. R. Kirsch and N. R. Morris, *Anal. Biochem.*, 1980, **105**, 361.
59 N. Jaffrezie-Renault, C. Martelet, Y. Chevelot and J. P. Cloarec, *Sensors*, 2007, **7**, 589.

